

# Approach to $3 \times 3$ Decoupling and Control of Thermomechanical Pulp Refiners

Daniel Berg  
daniel.berg@cit.chalmers.se

Anders Karlström  
anders.karlstrom@cit.chalmers.se

Chalmers University of Technology  
SE-412 92 Göteborg, Sweden

## Abstract

*Theories for the exact and approximative decoupling of  $2 \times 2$  transfer function matrices are well developed and readily available in the literature. Extended to a  $3 \times 3$  structure, decoupling approaches sometimes turn out to be somewhat complicated to perform. In this paper, a primary refiner is modeled using a linear  $3 \times 3$  system structure. In addition to consistency and motor load, refining zone temperature are regarded as outputs. The inputs that are used are production rate, dilution-water feed rate and hydraulic pressure.*

*Both approximative and exact dynamic decoupling are investigated and a sufficient condition for stability is given. It is found that the dynamic decoupling of  $3 \times 3$  systems can result in slow control action for the closed-loop system. Simplifications of the dynamic description are therefore introduced by reducing the system to a  $2 \times 2$  system and choosing the optimal inputs and outputs such that the relative gain array for the sub-diagonal elements is essentially negligible.*

## 1 Introduction

Significant improvements have been made in the paper-making process, as well as in the defibration of wood and pulp, during the last decade. New control strategies for refiners have been proposed and it is known that specific energy alone is insufficient when characterizing the refining process [18]. Recently, refiner control strategies have focused on new measurement techniques, such as plate gap and blow-line consistency measurements, to keep the quality as constant as possible [23]. Techniques for measuring temperature inside the refining zone have also been proposed as a complement to different measurement techniques [19], but the primary aim so far has been to use new knowledge relating to internal states to increase our understanding of the refining processes [5].

Although many theoretical approaches to the control of

TMP plants can be found in the literature [1, 6, 8], it is estimated that about 90% of all the installed advanced control systems are disconnected within a year [11].

The TMP system is a Multi-Input Multi-Output (MIMO) control system, a fact that appears to be handled in two ways. Either by disregarding it completely using several Single-Input Single-Output (SISO) loops, sometimes with additional heuristic information about some dominant interaction in the process, or by installing a model based control such as predictive control [7, 11]. Another method for obtaining a flexible control structure is to combine a simple controller with some kind of decoupling filter. This, however, requires some knowledge of the process dynamic associated with the interactions. The literature on the decoupling of  $2 \times 2$  systems is extensive [13, 24, 25] and the results are, for example, applied to distillation control [16]. In the case of general MIMO systems, research focus on the conditions for the existence of decoupling controllers [12] and numerically deduced precompensation filters and controllers [26].

In this paper, the decoupling strategies that are often used in  $2 \times 2$  systems [24] have been generalized to produce theories relating to a  $3 \times 3$  system. In Section 2, fundamentals relating to decoupling phenomena in refiner processes are considered. The results of the theories applied to refiner systems are presented in Section 3, together with a reduction of the system complexity from a  $3 \times 3$  system to a  $2 \times 2$  system.

## 2 Fundamentals

The approach proposed in this paper is based on the work presented by Eriksson et al. [9], where full-scale industrial TMP refiners were modeled and verified. From a system perspective, it was shown that a simplified, time-invariant model structure for two serially-linked refiners can be given by the relation

$$y_x = G_x(s)u_x, \quad x \in \{1, 2\} \quad (1)$$

where  $G_x(s)$  is the transfer-function matrix.

Most frequently, the input signal vectors  $u_x$ , see Fig. 1, relate to the chip and dilution-water feed rates, in addition to the hydraulic pressure applied to the stators [2]. The output

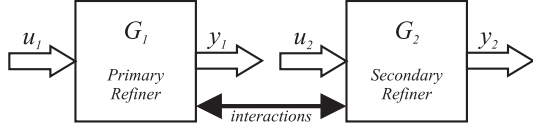


**Figure 1. The principal refiner-line structure.**

vector,  $y_x$ , can be the measured or estimated consistency [5] in the blow line, the motor load or other measurements like the temperature in the refining zone [21]. The refining process is thereby a typical MIMO system, with at least three inputs and a variable number of outputs. This implies that a number of different control strategies exist, depending on the process design.

In some processes, the hydraulic pressure is kept as constant as possible, while in other cases it is an input used for plate-gap control. When hydraulic pressure (or plate gap) is not assumed to be a constant input candidate, the  $G_x(s)$  is at least a  $3 \times 3$  system with several interactions, where the inputs affect more than one output. To control processes of this kind, it is important to have a global control approach and to reduce the interactions in the system.

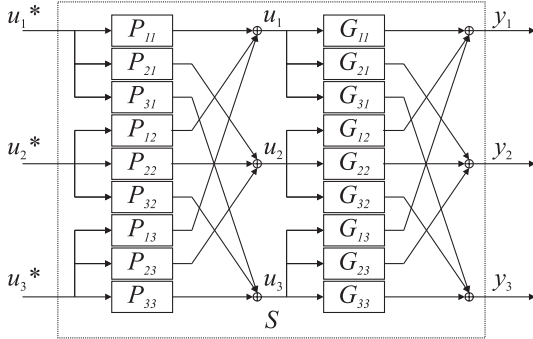


**Figure 2. Decoupled open system  $S = GP$ .  $G$  is the actual physical system (refiner) and  $P$  is the decoupling filter.**

One common procedure for reducing interactions is to introduce software-based decoupling filters  $P = [P_{ij}]_{3 \times 3}$ , see Fig. 2, so that a matrix  $S = GP$  is diagonal and non-singular, i.e.

$$S = \begin{bmatrix} S_{11} & 0 & 0 \\ 0 & S_{22} & 0 \\ 0 & 0 & S_{33} \end{bmatrix} \quad (2)$$

There are several ways to design  $P$ , whereof two are exact

decoupling, where  $S$  is chosen and  $P = G^{-1}S$  calculated, and approximate decoupling, where  $P$  is found by minimizing a cost function numerically.

The choice of the exact decoupled system,  $S^e$ , can be made theoretically in an infinite number of ways. One choice is

$$S_{ii}^e = \det(G)\Delta_{ii}^{-1}, \quad i \in \{1, 2, 3\} \quad (3)$$

where  $\Delta_{ij}$  are the cofactors of  $G$  [20]. The superscript  $e$  denotes exact decoupled. This is a generalization of the "optimal" choice for a  $2 \times 2$  system [24]. This choice is also known as simplified decoupling, as opposed to ideal decoupling [16, 25], where  $S_{ii}^e = G_{ii}$ .

The exact decoupling filter coefficients are then

$$P_{ij}^e = \frac{\Delta_{ji}}{\Delta_{jj}} \quad i, j \in \{1, 2, 3\} \quad (4)$$

implying that the diagonal elements are unity.

If stable first-order systems are assumed for the elements in  $G$ , i.e.

$$G_{ij} = \frac{K_{ij}}{T_{ij}s + 1}, \quad i, j \in \{1, 2, 3\} \quad (5)$$

where  $K_{ij}$  and  $T_{ij} > 0$  are the low-frequency gain and time constant respectively, a rule of thumb for stability can be formulated. The cofactors,  $\Delta_{ij}$ , and the determinant,  $\det(G)$ , are stable as  $G$  is stable and consequently  $P^e$  and  $S^e$  are stable, if the inverse of the diagonal cofactors, i.e.  $\Delta_{ii}^{-1}$ , is stable. Fulfilling the inequalities

$$\begin{aligned} |K_{kk}||K_{ll}| &> |K_{kl}||K_{lk}| \\ T_{kk}T_{ll} &< T_{kl}T_{lk}, & k, l \in \{1, 2, 3\} \\ T_{kk} + T_{ll} &< T_{kl} + T_{lk} & k \neq l \end{aligned} \quad (6)$$

thus produces a stable system [4].

Sometimes, the exact decoupling filter can be replaced by a constant filter matrix  $P^c$  which only decouples at a certain frequency,  $s = i\omega$ , i.e.  $P^c = P^e(i\omega)$ . Two interesting decoupling frequencies are  $\omega = 0$  rad/s and the cross-over frequency  $\omega = \omega_c$  rad/s, where the former is frequently used to avoid complex valued coefficients. This choice is applicable if the degree of coupling is frequency insensitive [4] and this can be determined visually by plotting the frequency-dependent relative gain array matrix (RGA) [15]

$$RGA(\omega) = G(i\omega) .* (G^{-1}(i\omega))^T \quad (7)$$

The sign ".\*" denotes element-wise multiplication and  $G$  is a transfer-function matrix. The RGA for the refiner system  $G$  is shown in Fig. 3, where the left-hand indices refer to RGA elements,  $(i, j) \Leftrightarrow RGA_{ij}$ . A high degree of coupling between the input  $i$  and the output  $j$  is indicated by  $RGA_{ij} \approx 1$ . Exact decoupled systems will have diagonal

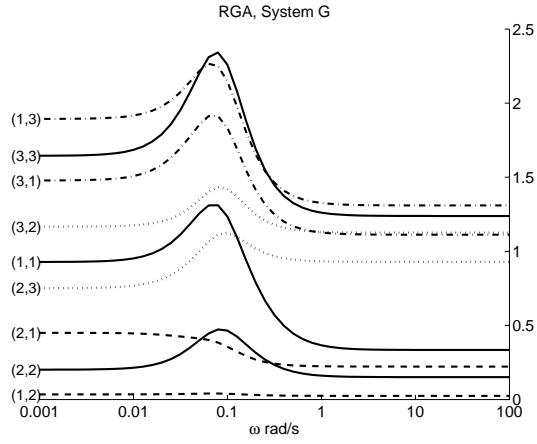


**Figure 3. RGA for a refining system process described by the transfer-function matrix  $G$ .**

elements  $RGA_{ii}(\omega) \equiv 1$  (solid lines) and sub-diagonal elements  $RGA_{ij}(\omega) \equiv 0$ ,  $i \neq j$ .

Exact decoupling becomes complex when the model order is increased. For a general transfer-function matrix,  $G = [G_{ij}]_{n \times n}$ , the order of  $\det(G)$  is  $m \cdot n \cdot n!$ , where  $m$  is the order of elements  $G_{ij}$ ,  $i, j \in \{1, 2, \dots, n\}$ . In the equivalent manner, the co-factors have the order  $m \cdot (n-1) \cdot (n-1)!$ . The high model order often implies numerical difficulties [4].

Designing an approximative decoupling filter

$$P_{ij}^n(s) = \begin{cases} \kappa_{ij} \frac{\sigma_{ij}s + 1}{\tau_{ij}s + 1}, & i \neq j \\ 1, & i = j \end{cases} \quad i, j \in \{1, 2, 3\} \quad (8)$$

is another way to create an analyzable system. The filter coefficients  $\kappa_{ij}$ ,  $\sigma_{ij}$ ,  $\tau_{ij}$  are calculated by minimizing a cost function

$$\min_{\kappa, \sigma, \tau} \sum_{i \neq j} \int_0^{\infty} y_{ij}(t) dt \quad (9)$$

where  $y_{ij}(t)$  is the unit step response of  $S_{ij}^n$ ,  $S^n = GP^n$  [24]. The superscript  $n$  denotes numerically optimized decoupled systems.

### 3 Results

As there are three inputs and several output candidates, the refiner system naturally becomes a  $n \times 3$  system. If a temperature vector containing measurement signals from eight sensors is used, the complete system has ten outputs. Using one of these sensors as an output, the structure can be described as a  $3 \times 3$  system. As can be seen in Fig. 4, which illustrates the low-frequency gains  $K_{ij}$  defined in Eq.

5, the use of the temperature sensor  $T_4$  or  $T_5$  as an output will produce a small gain from the dilution-water feed rate, while the other temperature sensors will produce a larger  $|K_{ij}|$ , which is not attractive from a decoupling perspective. When choosing the load as an output,  $|K_{ij}|$  will be large as well, while the consistency as an output will result in a small gain when the production rate and hydraulic pressure are changed. This information is valuable when trying to find sub-diagonal elements with small RGA values.

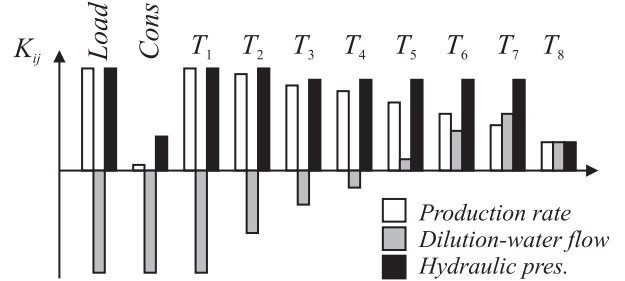


**Figure 4. Low-frequency gains for different elements in a  $10 \times 3$  system.**

In this paper, elements in the transfer-function matrix for the primary refiner are first-order models with one pole estimated using an output-error (OE) model [14].

$$\underbrace{\begin{bmatrix} T_5 \\ \text{Cons.} \\ \text{Load} \end{bmatrix}}_y = \underbrace{\begin{bmatrix} \frac{1}{9s+1} & \frac{0.1}{6s+1} & \frac{1.3}{15s+1} \\ \frac{-0.09}{30s+1} & \frac{-1}{17s+1} & \frac{0.2}{20s+1} \\ \frac{0.7}{6s+1} & \frac{-2.4}{5s+1} & \frac{1}{10s+1} \end{bmatrix}}_G \underbrace{\begin{bmatrix} \text{Prod.} \\ \text{Dilw.} \\ \text{Hydr.} \end{bmatrix}}_u \quad (10)$$

The low-frequency gains have been derived using PLS models [10] in order to verify stationary behavior, as measurements from a refiner are usually noisy and exhibit time variations [3], as well as direct-dependent dynamics [22]. The refiner system is clearly coupled with several interactions, which can also be seen in Fig. 3.

The need for decoupling can be verified by first applying a feedback control to each individual diagonal element  $G_{ii}(s)$ , as shown to the left in Fig. 5. The controllers  $F_{ii}(s)$  are assumed to be PI controllers. Each diagonal feedback loop is stable with a large stability margin, as the phase margin has been set at  $90^\circ$ . The crossover frequency  $\omega_c$  is approximately the inverse of the dominant time constant of  $G_{ii}$ . However, if the same control approach is applied to the MIMO system, Fig. 5, right, where all interactions are included, the closed-loop system becomes unstable. This is shown in Fig. 6, where the step responses of the input sensitivity function,  $(I + GF)^{-1}G$ , have been plotted. The use of the input sensitivity function, i.e.  $d_i$  to  $y_i$  in Fig. 5, and not the sensitivity function  $(I + GF)^{-1}$  is justified as distur-

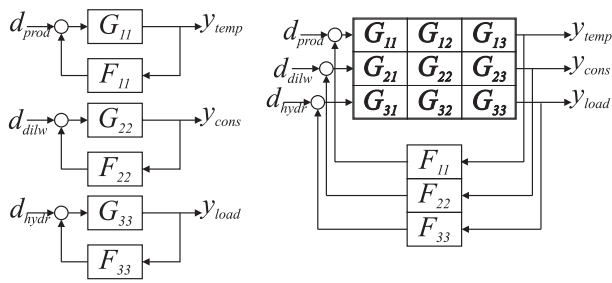


**Figure 5. SISO-loop design applied to diagonal elements, left, and the actual MIMO system, right.**

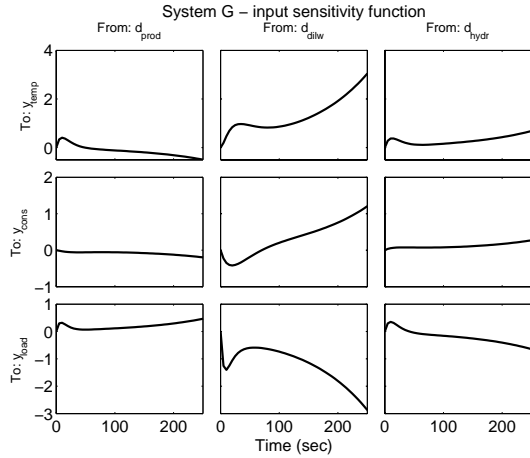


**Figure 6. Input sensitivity function for coupled system  $G$ .**

bances, such as chip and dilution-water feed disturbances, [2] are input disturbances.

For the open, exact decoupled system  $S^e$  in Eq. (3), step responses are shown in Fig. 7 and, as desired, sub-diagonal elements are close to zero. Frequency dependent RGAs for  $S^c$  and  $S^n$  are plotted in Fig. 8. As can be seen, both are decoupled for lower frequencies but not for higher frequencies — the former owing to the frequency dependence of the coupling, the latter as the optimization routine [17] has a problem converging properly due to the complexity of the optimal solution.

Step responses for the input sensitivity functions for the decoupled MIMO systems are shown in Fig. 9. Exact decoupling is plotted with a solid line, static decoupling with a dotted line and numerical decoupling with a dash-dotted line. The closed-loop systems are formed by applying the same control strategy as for  $G$ , see Fig. 5 but adjusting  $\omega_c$  to the inverse of the dominant time constant of the diagonal elements of the decoupled systems. The sub-diagonal

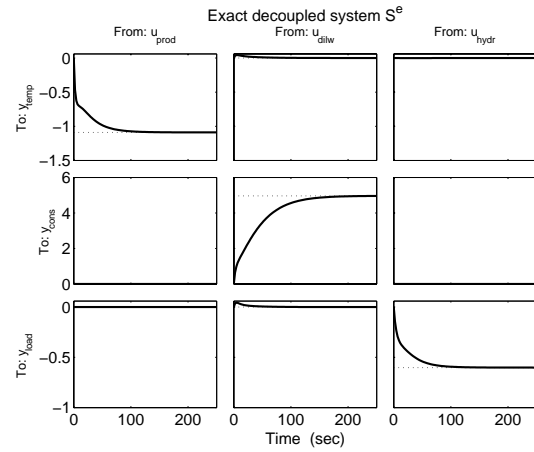


**Figure 7. System decoupled with exact decoupling.**

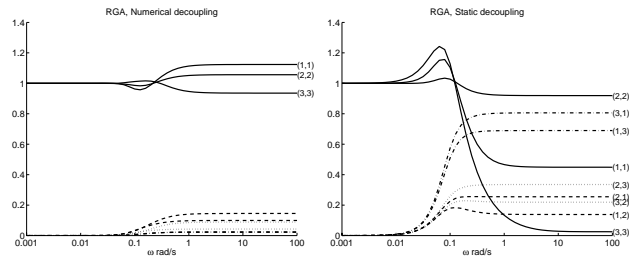


**Figure 8. RGA for numerically decoupled system, left and for static decoupling, right.**

elements of numerically and stationary decoupled systems have a transient response but negligible low-frequency gain, which is also indicated in Fig. 8. The scale in Fig. 9 is selected to emphasize the fact that numerically decoupled sub-diagonal elements also have transient responses.

Consequently, even though the filter can be designed, a more robust solution should also be considered as time-varying aspects can, for example, affect control robustness. Decoupling of the  $3 \times 3$  system does not solve the problem satisfactorily. Important time constants for the refiner are normally about 10 seconds, as can be seen in Eq. (10), while for the decoupled system in Fig. 7 the relevant time constant will be about 50–100 seconds. An examination of Fig. 4 reveals that the low-frequency gain using load as an output is high for all input signals. This is to be expected, as load is the "sum" of all the actions in the refiner. However, this also implies a high degree of coupling, see Fig. 3, where the elements with output  $(3, j)$ , i.e. load, are highly coupled. For systems with a high degree of coupling, removing the most coupled input and output signal according

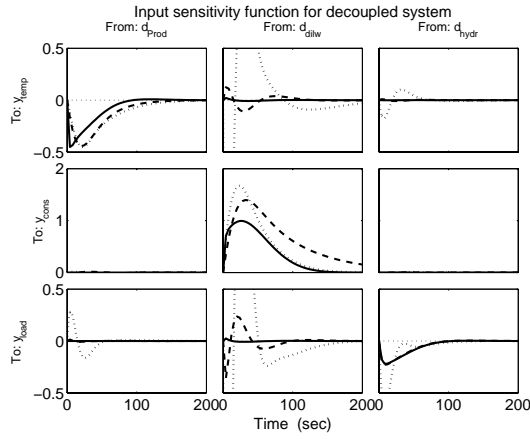


**Figure 9. Step response for input sensitivity function for decoupled systems. Exact decoupling, solid line, static decoupling, dotted line, and numerically decoupled, dash-dotted line.**

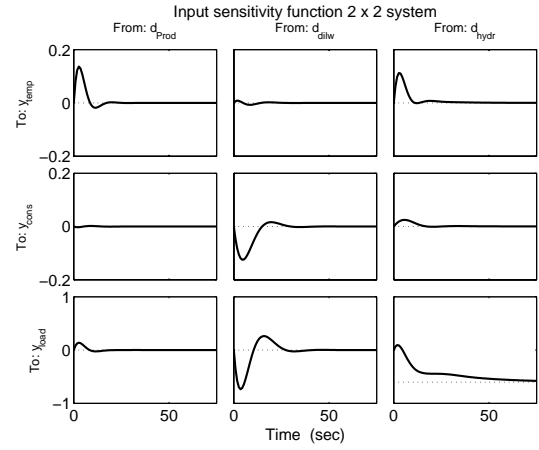


**Figure 10. Input sensitivity function for  $2 \times 2$  system. Hydraulic pressure and load excluded.**

to the RGA can be justified as a high degree of coupling also indicates that an output could be a linear combination of the other outputs and only contain redundant information.

The most favorable solution would be to find a transfer-function matrix which has zeros, or at least almost negligible elements, in its sub-diagonals and design a robust controller with simple decoupling filters. In refining processes with limited instrumentation, this is usually impossible, but, as the temperature profile is available, new opportunities for control design exist.

Removing the load is a good choice when it comes to obtaining a more naturally decoupled system, but, to achieve a  $2 \times 2$  system, an input must be removed as well. The choice is not obvious, but, from Fig. 4, it is perceptible that the subsystem

$$y = \begin{bmatrix} \text{Temp.} \\ \text{Conc.} \end{bmatrix} \quad u = \begin{bmatrix} \text{Prod. Rate} \\ \text{Dil. Water} \end{bmatrix} \quad (11)$$

or alternatively

$$y = \begin{bmatrix} \text{Temp.} \\ \text{Conc.} \end{bmatrix} \quad u = \begin{bmatrix} \text{Hydr. Pres.} \\ \text{Dil. Water} \end{bmatrix} \quad (12)$$

has a low degree of coupling, as the gain from production rate to consistency and from dilution-water feed rate to intermediate temperatures is very low [3], as can be seen in Fig. 4. However, the hydraulic pressure is also a possible choice for the input signal as the gain from hydraulic pressure to consistency is weak, even though the gain is higher than from the production rate. The dilution-water feed rate is the only input with a high gain to consistency, making it a clear input choice.

As can be seen in Fig. 10, the step response of the structure in Eq. 11, i.e with  $F_{33} \equiv 0$ , produces fast closed-loop dynamics and, moreover, the load will be indirectly controlled as it is correlated to temperature and consistency. However, this is not valid when the hydraulic pressure is changed. To also handle the steady-state error of load  $y_{load}$  from an input disturbance in hydraulic pressure  $d_{hydr}$  that can be seen in Fig. 10, a slow integrating controller could be used, i.e reinstalling  $F_{33}$ , but with slower control action. Step responses of the input sensitivity function can be seen in Fig. 11. When forming the closed loop input sensitivity function for the system in Eq. (11), however, the steady-state error from  $d_{hydr}$  to  $y_{load}$  is negative, whereas element  $G_{33}$  in the open loop system in Eq. (10) has a positive low-frequency gain. Thus, when forming the closed  $2 \times 2$  system low-frequency gains for remaining open elements can change sign.

It is also possible to modify the MIMO structure in order to fit the Eq. (12). This means that the controller structure becomes

$$F = \begin{bmatrix} 0 & 0 & F_{11} \\ 0 & F_{22} & 0 \\ F_{33} & 0 & 0 \end{bmatrix}$$

with the same inputs and outputs as indicated in Fig. 5. As can be seen in Fig. 12, step responses have been applied to the input sensitivity function according to Eq. (12) the closed-loop dynamics will be similar to those of the system in Eq. (11).

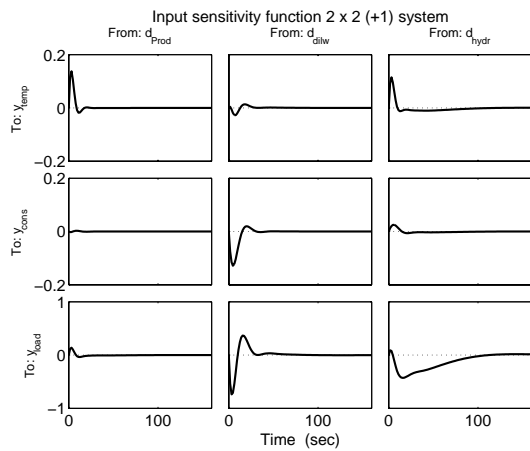


**Figure 11. Input sensitivity function for  $2 \times 2$  system though with controller  $F_{33}$  reinstalled with slow control action.**

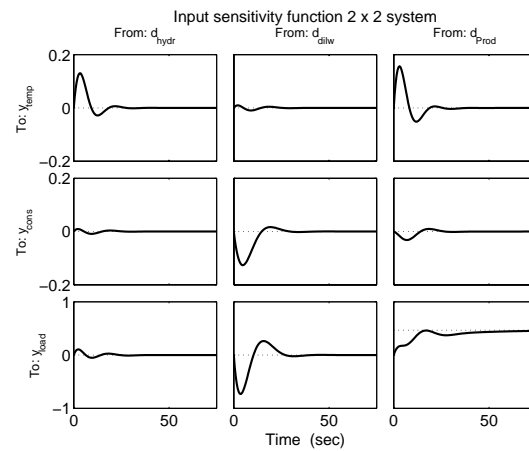


**Figure 12. Input sensitivity function for  $2 \times 2$  system. Production rate and load excluded.**

## 4 Conclusions

A control system for a refiner line must be very robust due to non-linear behavior such as plate wear, which causes changes in the time constants and gains over the running time period. A refiner line also has a multitude of interactions, further increasing the need for robustness and simplicity. Theoretically, the decoupling of  $3 \times 3$  systems is possible, but, as far as the refiner is concerned, it results in very large time constants due to the similarity between the low-frequency gains of the diagonal and sub-diagonal elements.

It is shown that exact decoupling is possible to derive, but this is unattractive for the control of the refiner due to the slow control action and the very high complexity of the system. Using numerical decoupling filters will significantly reduce the decoupling filter complexity compared with exact decoupling, but this results in slow control action for the resulting decoupled system as well. Static decoupling cannot be regarded as an alternative for decoupling, as the degree of coupling of the refiner is frequency dependent.

Moreover, for the refiners with installed temperature sensors, the reduction of the  $3 \times 3$  system to a  $2 \times 2$  system with temperature and consistency as outputs and production rate and dilution-water feed rate as inputs is shown to be the best choice. The high degree of correlation to temperature and consistency makes the information in the load excessive and input disturbances can therefore be handled by the  $2 \times 2$  feedback system. Output disturbances in the load, however, are not handled by the control system. However, the hydraulic pressure (or production rate) and load that are excluded from the  $2 \times 2$  system will not be ignored. A slow control action could be installed to handle the steady-state

error, but care should be taken as the low-frequency gain of remaining elements can change sign when forming the closed  $2 \times 2$  system and result in an unstable system in spite of the slow control action. The steady-state error can also be handled by implementing another temperature sensor from the array, for example  $T_7$ , instead of the load as an output signal. Thereby, a more robust controller could probably be designed.

Finally, the remaining input and output signals could be used by mill personnel to set the operation point, or can be used in a quality-control system working in another time frame.

If new instrumentation or soft sensors, such as residence time or a quality-related variable, are installed, a  $3 \times 3$  system with a lower degree of coupling could be formulated and the decoupling theories presented above could be applied.

## 5 Acknowledgement

The authors gratefully acknowledge funding by the Swedish Energy Agency.

## References

- [1] B. J. Allison, J. E. Ciarneillo, P. J.-C. Tessier, and G. A. Dumont. Dual adaptive control of chip refiner motor load. *Automatica*, 31(8):1169–1184, 1995.
- [2] D. Berg. Stability analysis in thermo-mechanical pulp refiners. Master's thesis, Chalmers University of Technology, SE-412 92, Göteborg, Sweden, 2002.
- [3] D. Berg. Energieeffektivisering i raffinieringsprocesser. Technical Report P-13838-1, Swedish Energy Agency, 2003. In Swedish.

- [4] D. Berg and A. Karlström. Theories for decoupling  $3 \times 3$ -systems with application to thermomechanical pulp refiners. Technical report, Department of Signals and Systems, Control and Automation Laboratory, Chalmers University of Technology, SE-412 92 Göteborg, Sweden, 2004.
- [5] D. Berg, A. Karlström, and M. Gustavsson. Deterministic consistency estimation in refining processes. In *International Mechanical Pulping Conference*, pages 361–366, Quebec City, Canada, 2 – 5 June 2003.
- [6] D. Di Ruscio, J. G. Balchen, A. Holmberg, and P. H. Frisenberg. Experience with nonlinear model based control strategy applied to a two stage TMP plant. In *Control Systems*, pages 282–288, Stockholm, Sweden, 31 May - 2 June 1994.
- [7] H. Du and G. A. Dumont. Constrained multivariable control of a wood chip refiner. In *13th Triennial World Congress, San Francisco, USA*, pages 349–354. IFAC, 1996.
- [8] G. A. Dumont and K. J. Åström. Wood chip refiner control. *IEEE Control Systems Magazine*, 8(2):32–43, 1988.
- [9] K. Eriksson, A. Karlström, F. Rosenqvist, and D. Berg. The impact of different input variables in a twin disc refiner line. In *Control Systems*, pages 229–233, Stockholm, Sweden, 2002.
- [10] P. Geladi and B. R. Kowalski. Partial least-squares regression: A tutorial. *Analytica Chimica Acta*, 185:1–17, 1986.
- [11] J. Lidén. Quality control of single stage double disc chip refining. Technical report, FSCN in the Department of Natural and Environmental Sciences, Mid Sweden University, SE-851 70 Sundsvall, Sweden, 2003.
- [12] C.-A. Lin. Necessary and sufficient conditions for existence of decoupling controllers. In *Proceedings of the 34th Conference on Decision & Control*, New Orleans, LA, 1995.
- [13] A. Linnemann and R. Maier. Decoupling by precompensation while maintaining stabilizability. *IEEE Transaction on Automatic Control*, 38(4):629–632, April 1993.
- [14] L. Ljung. *System Identification, Theory for the user*. Prentice Hall PTR, second edition, 1999.
- [15] P. Lundström and S. Skogestad. Opportunities and difficulties with  $5 \times 5$  distillation control. *Journal of Process Control*, 5(4):249–261, 1995.
- [16] W. L. Luyben. Distillation decoupling. *AIChE Journal*, 16(2):198–203, March 1970.
- [17] The Mathworks, 3 Apple Hill Drive, Natick, MA 01760-2098. *Built-in Manual for Matlab Release 13 with Service Pack 1*.
- [18] K. Miles. Refining intensity and pulp quality in high-consistency refining. *Paperi ja Puu — Paper and Timber*, 72(5):508–514, 1990.
- [19] K. Moseby, K.-A. Kure, G. Fuglem, and O. Johansson. Use of refining zone temperature measurements for refiner control. In *International Mechanical Pulping Conference*, pages 481–488, Helsinki, Finland, 4-8 June 2001.
- [20] L. Råde and B. Westergren. *Mathematics Handbook for Science and Engineering*. Studentlitteratur, Lund, Sweden, third edition, 1995.
- [21] F. Rosenqvist, K. Eriksson, and A. Karlström. Time-variant modelling of TMP refining. In *IEEE IAS Workshop on Advanced Process Control*, pages 37 – 42, Vancouver, Canada, May 2001.
- [22] F. Rosenqvist, A. Karlström, and K. Eriksson. Parameter estimation in processes with direction-dependent dynamics. In *3rd International Conference on Identification in Engineering Systems*, Swansea, UK, April 2002.
- [23] B. Strand. Model based control of high consistency refining. *Tappi Journal*, 79(10):140–146, 1996.
- [24] B. Thomas. Identification, decoupling and PID-control of industrial processes. Technical Report 204, Department of Signals and Systems, Control and Automation Laboratory, Chalmers University of Technology, SE-412 92 Göteborg, Sweden, 1990.
- [25] M. Waller, J. B. Waller, and K. V. Waller. Decoupling revisited. *Industrial and Engineering Chemistry Research*, 42:4575–4577, 2003.
- [26] Q.-G. Wang, Y. Zhang, and M.-S. Chiu. Non-interacting control design for multivariable industrial processes. *Journal of Process Control*, 13:253–265, 2003.